Supplementary Information - Sizing individual dielectric nanoparticles with quantitative differential interference contrast microscopy

Samuel Hamilton,[1] David Regan,[1] Lukas Payne,[1,2] Wolfgang Langbein,[2,*] and Paola Borri[1,†]

[1] *School of Biosciences, Cardiff University, Cardiff, UK*
[2] *School of Physics and Astronomy, Cardiff University, Cardiff, UK*

(Dated: February 4, 2022)

S1. QDIC OPTIMIZATION AND CALIBRATION

As discussed in the main paper, to determine the SNR (and thus the SN pair), the integrated phase area A_ϕ^{m} is evaluated at many positions not showing a visible particle in the image, and its histogram is fitted with a Gaussian to determine its standard deviation σ, as can be seen in Fig. S1.

Fig. S2 shows the dependence of the measured phase area A_ϕ^{m} and the SNR on κ and r_i for the 0.75 NA objective. Similarly Fig. S3 shows the same for the 1.27 NA objective, both at $\psi = 30°$. A similar behaviour to that of the 1.45 NA objective is seen. However, saturation occurs at (10^5,4) for the 0.75 NA objective, while for the 1.27 NA objective saturation occurs at the same values as for the 1.45 NA objective. The pairs chosen for the SN are $(1, 1)$ and $(1, 1.5)$ for 0.75 NA and 1.27 NA, respectively, while the SE pair was $(100, 2)$ for both.

Complementing Fig. 1 for the other objectives used, we show here representative differential phase images $\delta(\mathbf{r})$ for PS beads of nominal 100 nm radius deposited onto glass and embedded in silicon oil, using the 0.75 NA microscope objective (Fig. S5a) and using the 1.27NA objective (Fig. S6a). The corresponding retrieved optical phase $\phi(\mathbf{r})$ for different κ is shown in Fig. S5b-d and Fig. S6b-d, as indicated.

To show the remarkable absence of blemishes or vignetting in the DIC contrast as compared to individual DIC images, we show the I_+ image corresponding to Fig. 1a in Fig. S7.

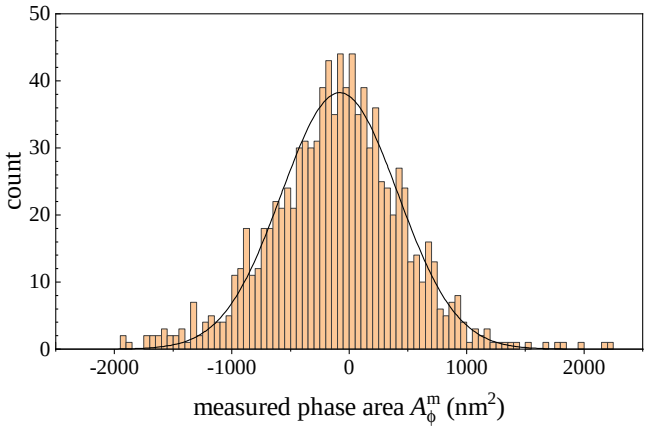

FIG. S1. Histogram of the A_ϕ^{m} distribution at background points for PS beads mounted in silicone oil, imaged with the 0.75NA objective and analysed using $\kappa = 10^5$ and $r_i = 4$. The line shows the Gaussian function applied to find the standard deviation of the distribution, which in this case was $\sigma = 495.8 \pm 5.3\,\mathrm{nm}^2$.

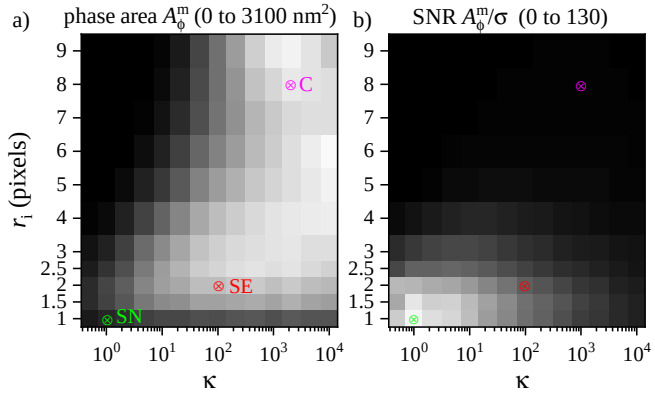

FIG. S2. Phase area A_ϕ^{m} (a, $m = 0$ to $M = 3100\,\mathrm{nm}^2$) and SNR $A_\phi^{\mathrm{m}}/\sigma$ (b, $m = 0$ to $M = 130$) as function κ and r_{i} for the 0.75 NA objective and $\psi = 30°$. The chosen (κ, r_{i}) pairs SN, SE, and C are indicated.

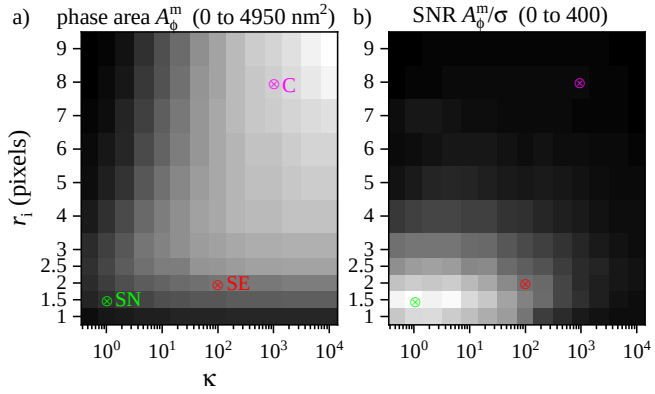

FIG. S3. Phase area A_ϕ^{m} (a, $m = 0$ to $M = 4950\,\mathrm{nm}^2$) and SNR $A_\phi^{\mathrm{m}}/\sigma$ (b, $m = 0$ to $M = 400$) as function κ and r_{i} for the 1.27 NA objective and $\psi = 30°$. The chosen (κ, r_{i}) pairs SN, SE, and C are indicated.

* langbeinww@cardiff.ac.uk
† borrip@cardiff.ac.uk

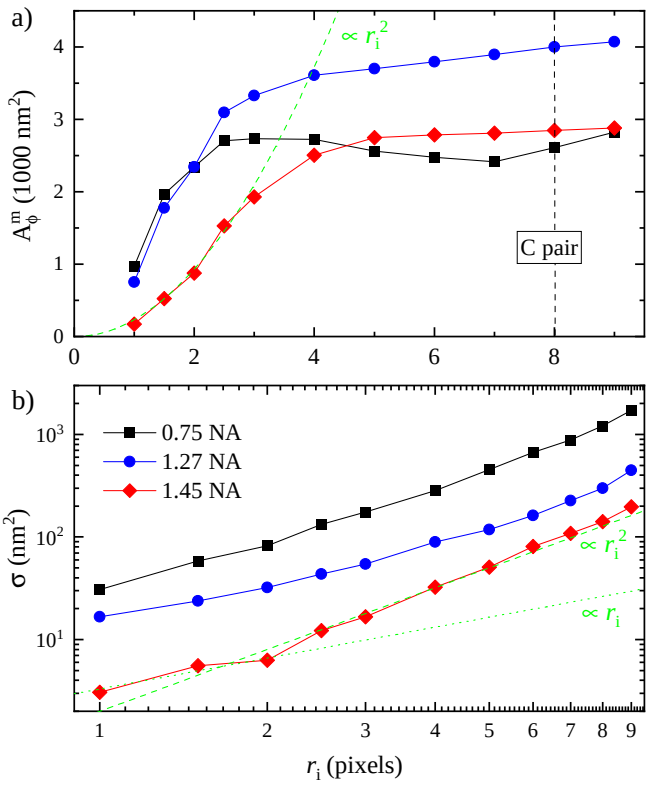

FIG. S4. (a) phase area A_ϕ^m and (b) standard deviation of the background fluctuations σ versus inner radius r_i, for $\kappa = 1000$ and the three objectives as labelled, for 100 nm radius PS beads in silicone oil. The r_i used for the C-pair is indicated in (a). A linear and a quadratic scaling with r_i is shown by green dashed lines. Note that the data in (a) for the different objectives refers to different beads.

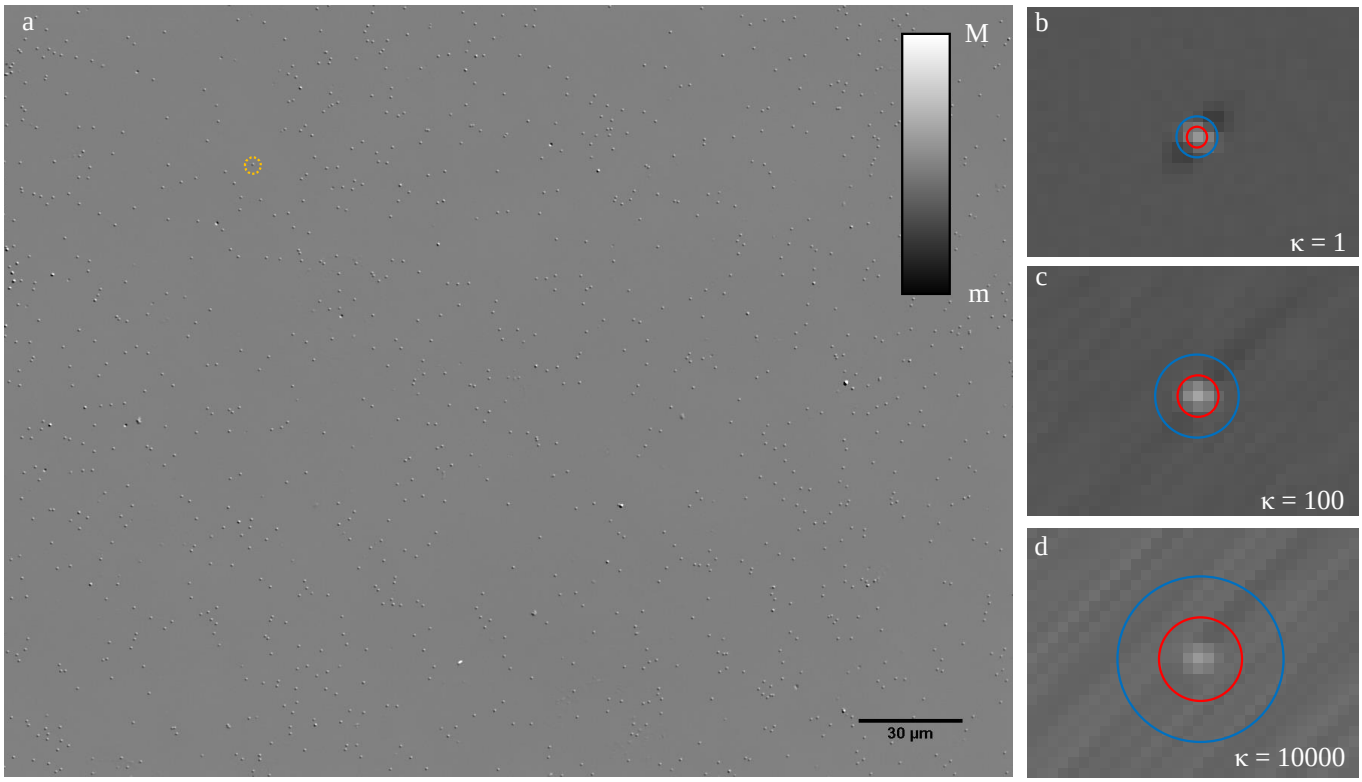

FIG. S5. qDIC on individual PS beads of nominal 100 nm radius deposited onto a glass surface in silicon oil, imaged with 0.75 NA and a phase offset of $\psi = 30°$. a) $\delta(\mathbf{r})$ on a grey scale as shown, from $m = -15$ mrad to $M = 15$ mrad. $\phi(\mathbf{r})$ images showing a region of (6.92×5.19) µm^2 around a selected bead indicated by the dashed circle are shown for $\kappa = 1$ (b, $m = -5$ mrad to $M = 10$ mrad), $\kappa = 100$ (c, $m = -10$ mrad to $M = 21$ mrad), and $\kappa = 10000$ (d, $m = -21$ mrad to $M = 30$ mrad), with the red and blue circles having the radii r_i and $2r_\mathrm{i}$, respectively, with $r_\mathrm{i} = 1, 2, 4$ pixels in b,c,d, respectively, representing different integration areas A_i and A_b used in the analysis (see main paper).

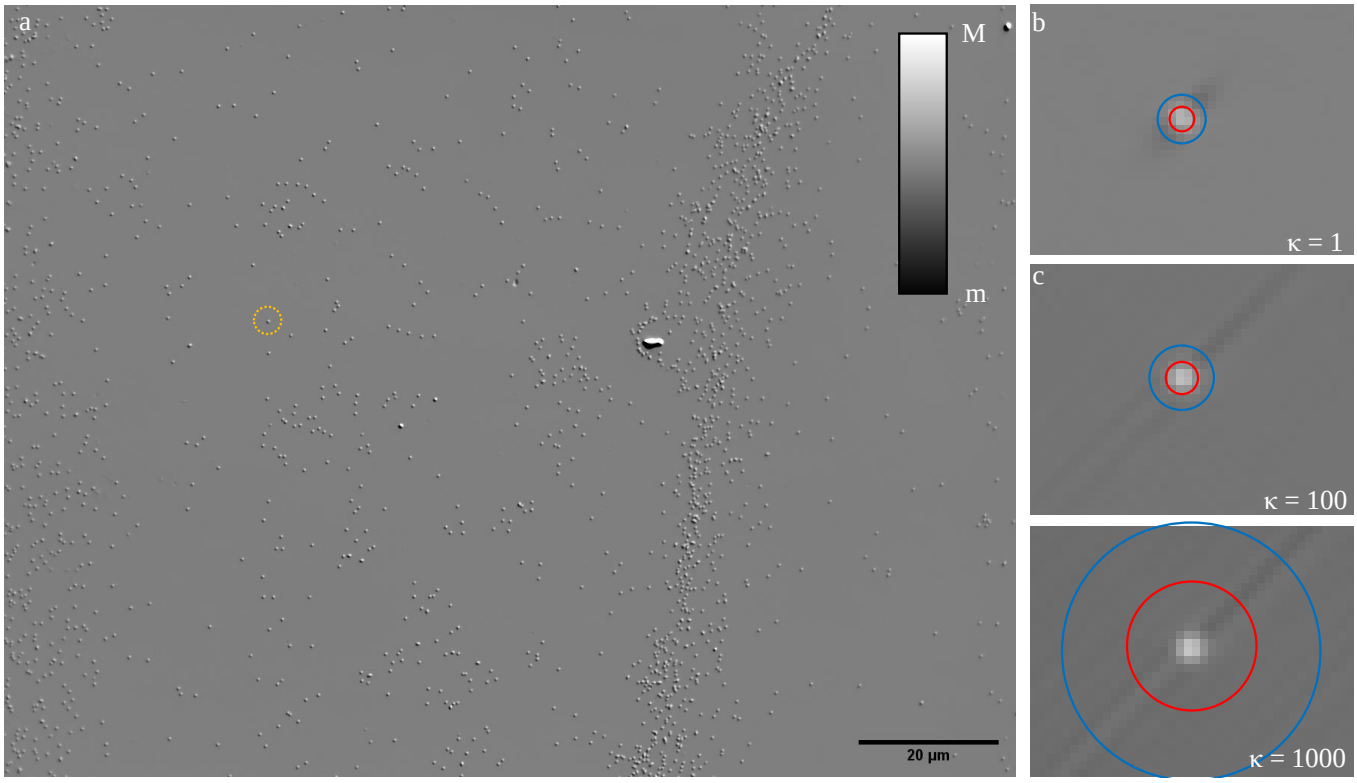

FIG. S6. qDIC on individual PS beads onto a glass surface in silicon oil, imaged with 1.27 NA and a phase offset of $\psi = 30°$. a) $\delta(\mathbf{r})$ on a grey scale as shown, from $m = -50.3$ mrad to $M = 50.9$ mrad. $\phi(\mathbf{r})$ images showing a region of $(4.30 \times 3.33)\,\mu\text{m}^2$ around a selected bead indicated by the dashed circle are shown for $\kappa = 1$ (b, $m = -41.1$ mrad to $M = 41$ mrad), $\kappa = 100$ (c, $m = -49.4$ mrad to $M = 60.4$ mrad), and $\kappa = 1000$ (d, $m = -39.2$ mrad to $M = 59.3$ mrad), with the red and blue circles having the radii r_i and $2r_\text{i}$, respectively, with $r_\text{i} = 1.5, 2, 8$ pixels in b,c,d, respectively, representing different integration areas A_i and A_b used in the analysis.

FIG. S7. I_+ image of the PS bead sample mounted in silicone oil ($m = 2600$ to $M = 3400$ counts) at the same region shown in Fig. 1 imaged using the 1.45 NA objective and a phase offset of $\psi = 30°$.

S2. PS BEAD REFRACTIVE INDEX

The refractive index (RI) of the PS beads was found by obtaining the average integrated phase area for PS beads mounted in water oil (WO) and silicon oil (SO), and using the fact that the phase area is proportional to the refractive index difference between medium and bead (Eq. 11). Firstly, we fitted the A_ϕ^{m} distributions measured at $\psi = 30°$ and analysed with the C pair of (κ, r_{i}) parameters for each microscope objective, using a Gaussian fit. The resulting mean $\bar{A}_\phi^{\mathrm{m}}$ and the error of the mean $\hat{A}_\phi^{\mathrm{m}}$ for each mounting medium and objective were used to retrieve the index of the beads as

$$n_{\mathrm{p}} = \frac{\bar{A}_\phi^{\mathrm{m}}(\mathrm{SO}) - \bar{A}_\phi^{\mathrm{m}}(\mathrm{WO})}{1 - n_{\mathrm{so}}/n_{\mathrm{wo}}} \tag{S1}$$

The corresponding data and linear extrapolation are shown in Fig. S8. The error of n_{p} was found using error propagation from the errors of the mean, yielding $n_{\mathrm{p}} = 1.5884 \pm 0.0005$, $n_{\mathrm{p}} = 1.5981 \pm 0.0015$, $n_{\mathrm{p}} = 1.5984 \pm 0.0013$ for the 0.75 NA, 1.27 NA, and 1.45 NA objectives, respectively. This matches well with the expected RI of 1.59, hence this value was used as the PS bead RI throughout the analysis.

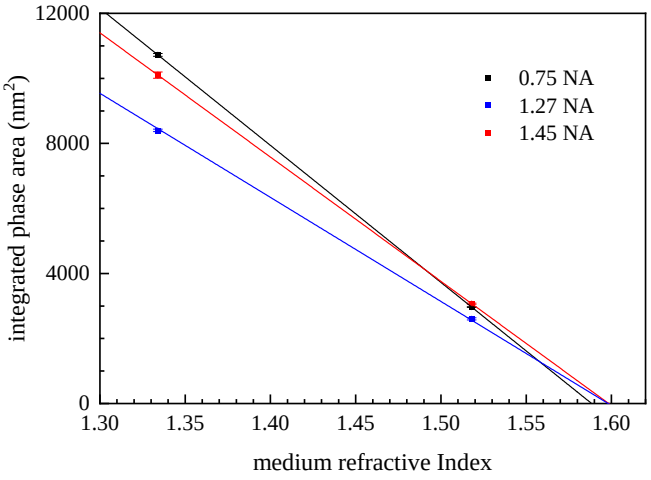

FIG. S8. Mean $\bar{A}_\phi^{\mathrm{m}}$ and standard deviation of the mean $\hat{A}_\phi^{\mathrm{m}}$ of the measured phase area A_ϕ^{m} of PS beads found for the 0.75 NA (black), 1.27 NA (blue), and 1.45 NA (red) objectives, with the linear extrapolation used in Eq. S1 to find the refractive index of the PS beads.

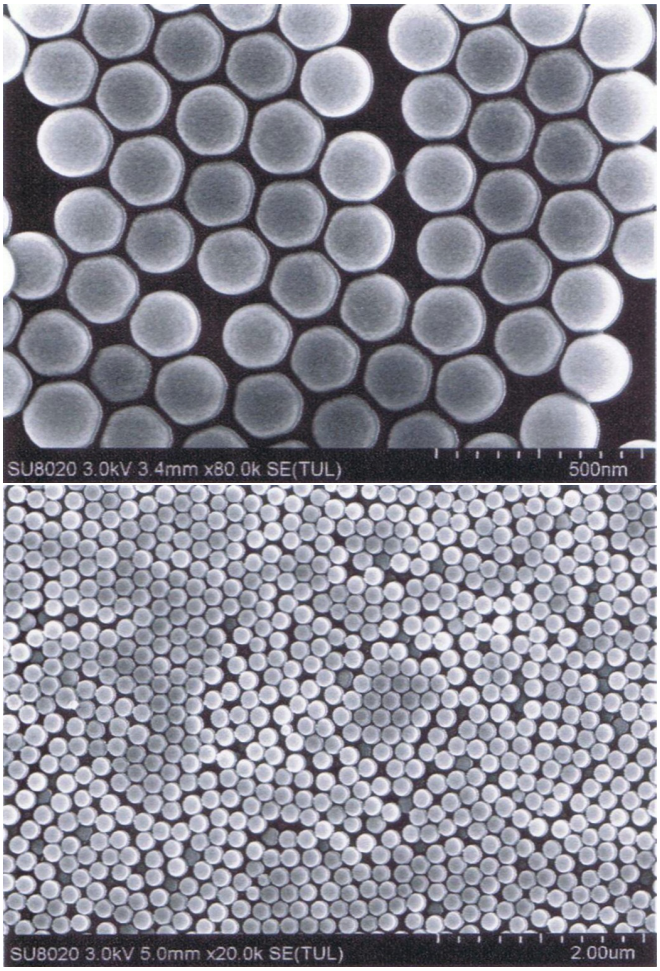

FIG. S9. Scanning electron microscopy characterization of the 100 nm radius PS beads from the manufacturer.

S3. PS BEAD CHARACTERIZATION

i. 100 nm radius PS beads

The PS beads were purchased from Alpha Nanotech, Colloidal PS Beads NP-PA07CPSX78, Batch number # 03182. They have a nominal radius of 100 nm and a coefficient of variance (cv) below 3%, which is the standard deviation of the radius. They were selected for their small cv compared to other manufacturers. We purchased a bottle of 10 ml at a concentration of 10mg/ml, in Milli-Q water. Their zeta potential was specified as -18 ± 4 mV.

Scanning electron microscopy (SEM) images from the manufacturer are shown in Fig. S9, indicating the high uniformity of the ensemble. The apparent hexagonal shape is an imaging artefact of the secondary electron collection for the dense ensembles, as can be seen from the round shape observed in absence of a nearby sphere. Note that 3% cv has to be multiplied by $\sqrt{8 \ln 2} \approx 2.355$ to obtain the full width at half maximum (FWHM) of 7%. From the SEM images, an average diameter of 190 nm is measured using closed packed rows of particles in the im-

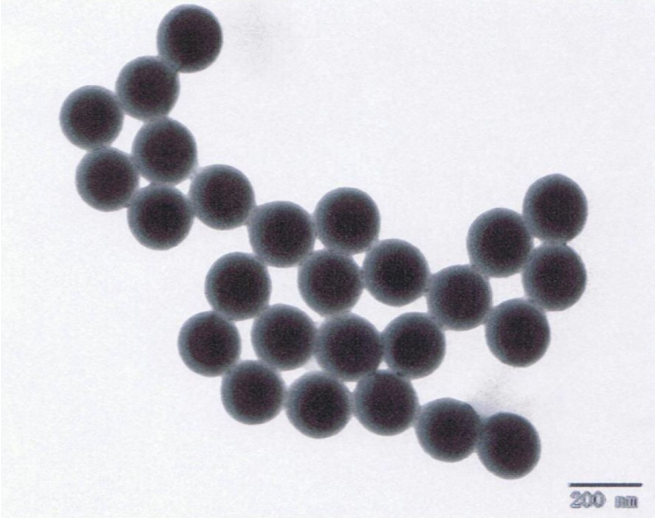

FIG. S10. Transmission electron microscopy characterization of the 100 nm radius PS beads from the manufacturer.

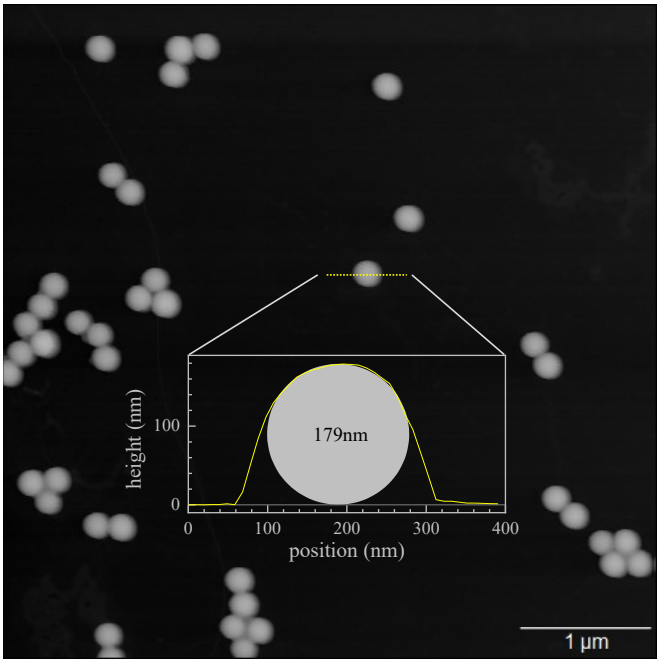

FIG. S11. a) AFM image of the 100 nm radius PS bead sample (gray scale from $m = 0$ nm to $M = 300$ nm). The height profile across a bead indicated by the dotted yellow line is given in the inset with a 1:1 aspect ratio, overlaid onto a 179 nm diameter spherical shape.

ages.

Transmission electron microscopy (TEM) image from the manufacturer is shown in Fig. S10. The mean diameter of the particles is measured to be 187 nm, corresponding to a radius of 93.5 nm, and the cv is measured to be 2.1%. Notably, electron microscopes can have calibration errors in the range of a few percent, similar to the differences seen between the TEM and SEM data.

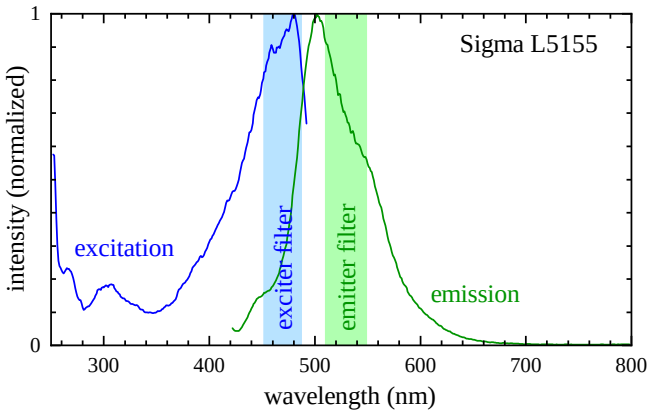

FIG. S12. Fluorescence excitation and emission spectra of the 15 nm radius PS beads, together with the transmission ranges of exciter and emitter filter used for fluorescence imaging.

Atomic force microscopy (AFM) images were taken by us using a Bruker Dimension Icon, in peakforce tapping mode using a scanasyst-air tip (silicon nitride, tip radius 2 nm, sidewall angles 15, 17.5, and 25 degrees). The samples of PS beads on a coverslip were prepared using the same concentration and procedure as for the DIC samples, but ending before oil immersion. Fig. S11 shows a representative result, together with a height profile of a selected PS bead consistent with an approximately spherical shape. The height distribution of all beads was measured to be 179 ± 6.7 nm. This is some 5% smaller than the SEM and TEM results, which might be explained by the beads preferentially attaching with their lower curvature side on the surface, so that the height measured is the smaller diameter of a slightly elliptical bead.

Finally, we have measured the PS beads with DLS (Malvern Zetasizer Nano ZS – the dispersions measured were the same as those used for the drop casting the AFM and qDIC sample), reporting a cumulant z-mean of 183 nm and a polydispersity index (pdi) of 0.22. This is consistent with the other characterization considering the typical errors of DLS measurements [1].

ii. 15 nm radius PS beads

Fluorescently labelled PS beads of nominally 15 nm radius were purchased from Sigma Aldrich, product number L5155. The manufacturer specifications state that they are made of carboxylate-modified polystyrene, are fluorescent yellow-green in aqueous suspension, have a mean diameter 20-40 nm, and a fluorescence excitation at 470 nm and emission at 505 nm.

We have measured the excitation and emission spectra using a spectrophotometer (Cary Eclipse) with 5 nm spectral resolution, as shown in Fig. S12. For fluorescence microscopy we used a Semrock GFP-A-Basic-NTE filter cube with an exciter filter transmitting the wavelength range 452-487 nm, and an emitter filter transmitting the

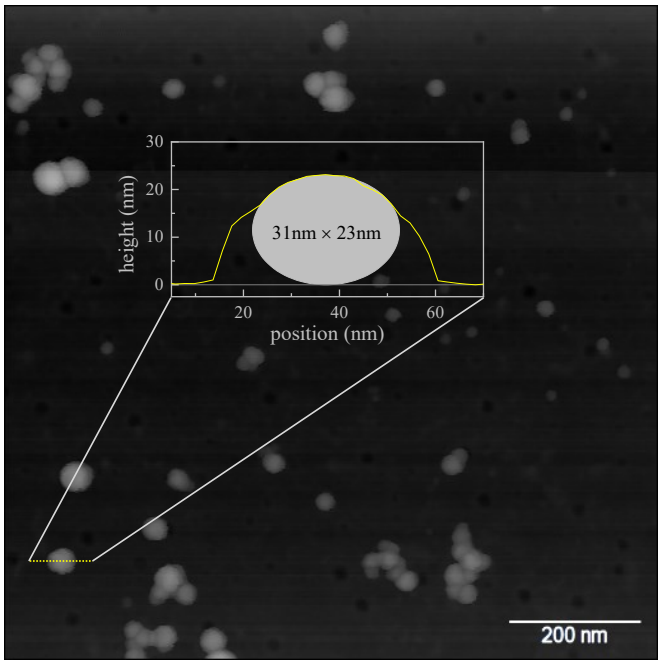

FIG. S13. AFM image of the 15 nm nominal radius PS bead sample ($m = 0$ nm to $M = 50$ nm). The height profile across a bead indicated by the dotted yellow line is given in the inset with a 1:1 aspect ratio, overlaid onto a (23×31) nm^2 elliptical shape.

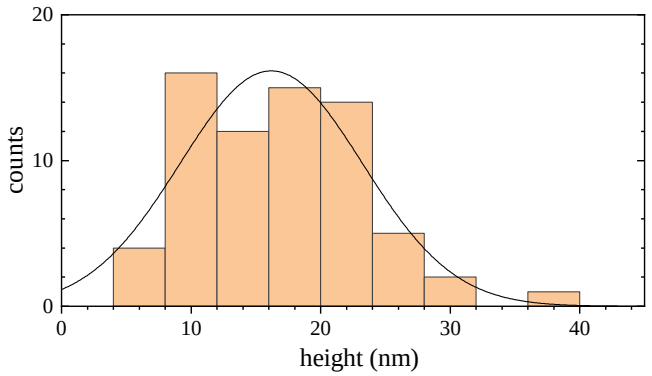

FIG. S14. AFM height distribution of the 15 nm radius bead sample, with a Gaussian fit of mean and standard deviation 16 ± 7 nm.

range 510-549 nm, as indicated in Fig. S12. Notably, the excitation used in DIC is not exciting fluorescence.

AFM images of the PS beads on a coverslip were taken, using the same concentration and procedure as for the DIC samples was used, but ending before oil immersion. Fig. S13 shows a representative result, together with a height profile of a selected PS bead of 23 nm height. The top curvature radius of this bead is 18 nm, which is 6.5 nm more than expected for a spherical particle of this height. The tip radius is specified as 2 nm, so that this result indicates flat-lying non-spherical beads, see the ellipse in the inset.

The height distribution of the beads visible in a few AFM images was measured and is shown in Fig. S14, having a broad distribution, with 16 nm mean and a cv of 44%.

DLS measurements provided a cumulant z-mean of 24 nm and a pdi of 0.52, which indicates a size distribution with a cv of about 52%, but there are caveats of this quantification [1]. The larger average size in DLS can be attributed to a non-spherical shape and larger weight of larger particles in the z-mean of DLS combined with the significant size distribution.

S4. CORRECTION FACTORS AND POLYSTYRENE BEAD RADII

The effective radius R_n of an n bead aggregate for the analysis which measures the volume is calculated from the sum of single particle volumes V_1,

$$R_n = \sqrt[3]{n\frac{3V_1}{4\pi}}, \tag{S2}$$

resulting in $R_n = \sqrt[3]{n}R_1$. To calculate the standard deviation of R_n, we start by assuming independent variations of the constituting particles. Noting that the volume standard deviation of a single particle is given

$$\sigma_1^V = \sigma_1 \left.\frac{\partial V}{\partial R}\right|_{R_1}. \tag{S3}$$

we find that adding the independent deviations on n particles, produces a volume deviation of an n-particle aggregate of

$$\sigma_n^V = \sigma_1\sqrt{n}\left.\frac{\partial V}{\partial R}\right|_{R_1}, \tag{S4}$$

and we can calculate the corresponding radius deviations as

$$\sigma_n = \left.\frac{\partial R}{\partial V}\right|_{R_n}\sqrt{n}\left.\frac{\partial V}{\partial R}\right|_{R_1}\sigma_1. \tag{S5}$$

Now, using the fact that $\partial V/\partial R \propto R^2$, we find

$$\sigma_n = \sigma_1\sqrt{n}\frac{R_1^2}{R_n^2} = \sigma_1\sqrt{n}\left(\sqrt[3]{n}\right)^{-2} = \frac{\sigma_1}{\sqrt[6]{n}}. \tag{S6}$$

Fig. S15 to Fig. S19 show the correction factor ϱ and radius R distributions for the WO and SO mounted samples imaged using the 0.75 NA and 1.27 NA objectives at $\psi = 30°$, and analysed using the SN or SE pair. Also shown are ϱ and R distributions for the WO mounted sample imaged using the 1.45 NA objective at $\psi = 30°$. Correction factors for these conditions range from $\rho = 1.23$ to $\rho = 7.07$, with the resulting single bead radii found to be between 97.2 nm and 102 nm, and standard deviations between 2.5 nm and 5.5 nm. The values for B (see Eq. 15 in the main paper) were found to be between 11,920 and 113,953 for these fits, and the values for λ were found to be between 0.005 and 0.12.

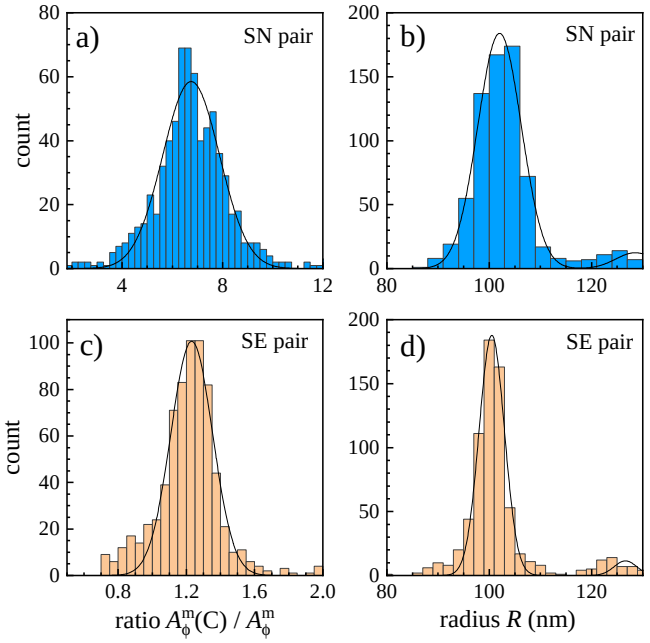

FIG. S15. Histograms of the correction factors ϱ obtained for the 0.75 NA objective and water oil mounted PS bead sample for the (κ, r_i) pair SN (a) and SE (c). Histograms of the resulting bead radii R, after the mean correction factor was applied, for the SN (b) and SE (d) pair.

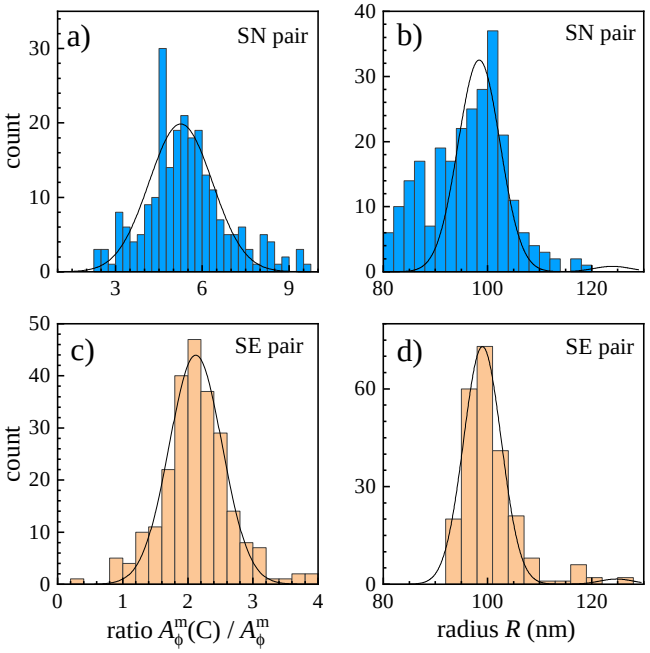

FIG. S16. As Fig. S15, but for the 1.27 NA objective.

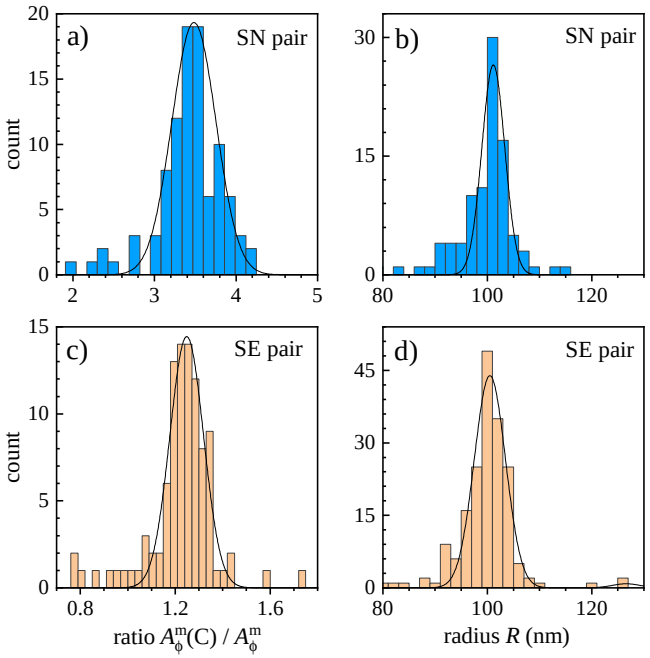

FIG. S17. As Fig. S15, but for the 1.45 NA objective.

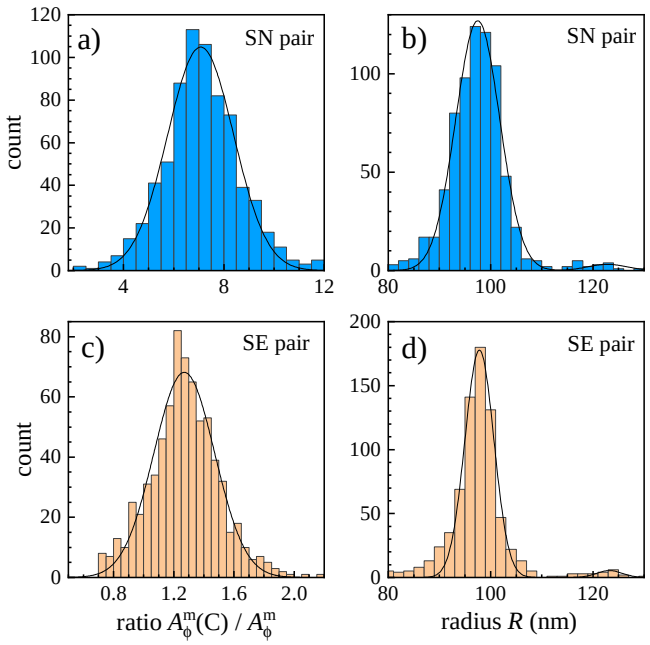

FIG. S18. As Fig. S15, but for silicone oil mounted PS bead sample.

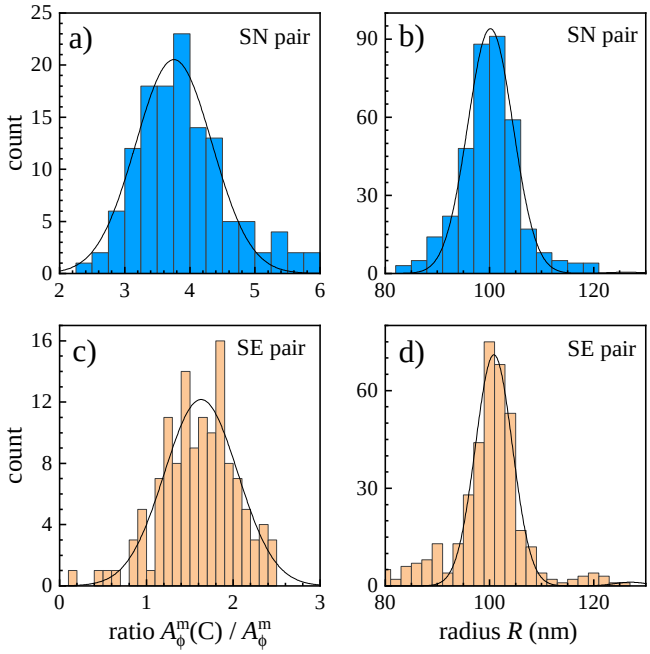

FIG. S19. As Fig. S18, but for the 1.27 NA objective.

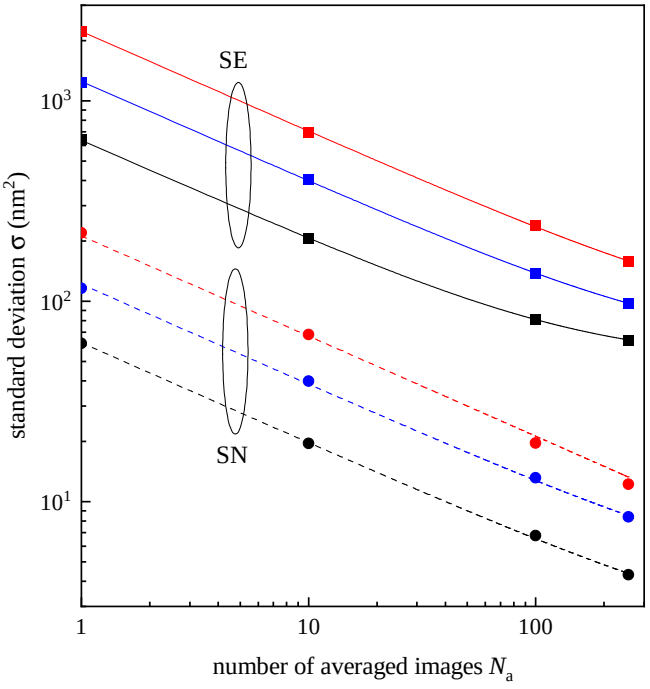

FIG. S20. Standard deviation σ, from the distribution of A_ϕ^m in regions of the sample without PS beads, versus the number of averages N_a for PS beads mounted in silicone oil imaged using the 0.75 NA objective and phase offsets ψ of 30° (black), 60° (blue), and 90° (red).

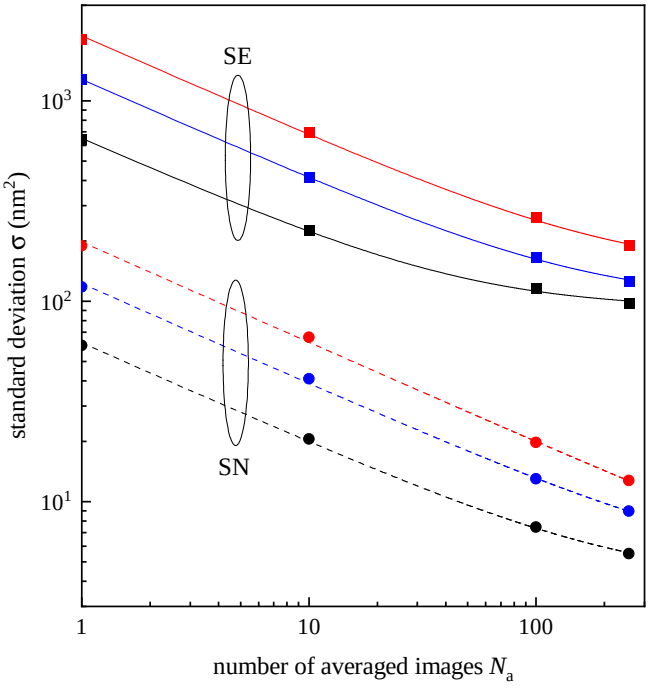

FIG. S21. As Fig. S20, but for the water oil mounted sample.

S5. BACKGROUND AND SHOT NOISE

In order to determine the background transmission factor η at $\phi = 0°$ for each objective, stacks of 256 images were obtained at angles ranging from $\phi = 90°$ to $-90°$ for all objectives at increasing lamp intensities. The average modal intensity for each stack $\langle I_\phi \rangle$ was extracted, and the one at $\phi = 0°$ was giving the median background intensity, $\langle I_0 \rangle$. For the (0.75, 1.27, 1.45) NA objectives, we measured $\langle I_0 \rangle = (48.82, 37.33, 46.77)$ counts, respectively, for $\langle I_{90} \rangle \approx 3000$ counts. We note that the digitization offset of the camera (192 counts) was subtracted from all images before any further processing, so that the pixel values are proportional to the detected photoelectrons. The intensities at angles of $\psi = 20°$, $\psi = 30°$, $\psi = 60°$, and $\psi = 90°$ for each objective were then used to find the background fraction f as

$$f(\psi) = \frac{\langle I_0 \rangle}{\langle I_\psi \rangle - \langle I_0 \rangle}, \tag{S7}$$

determining the background transmission factor as

$$\eta = f(\psi)\frac{1 - \cos(\psi)}{2}. \tag{S8}$$

The resulting values found for f and η for each objective are given in Table S1.

Fig. S20, Fig. S21, Fig. S22 and Fig. S23 show the dependence on the number of averages per image stack of the standard deviation σ, from the distribution of A_ϕ^m measured in regions of the sample without PS beads, for the 0.75 NA and 1.27 NA objectives. A dependence similar to that for the 1.45 NA objective is seen, and the resulting values of σ_s and σ_b for samples in water oil and silicone oil is summarised in Table 1. Fig. S24 shows the

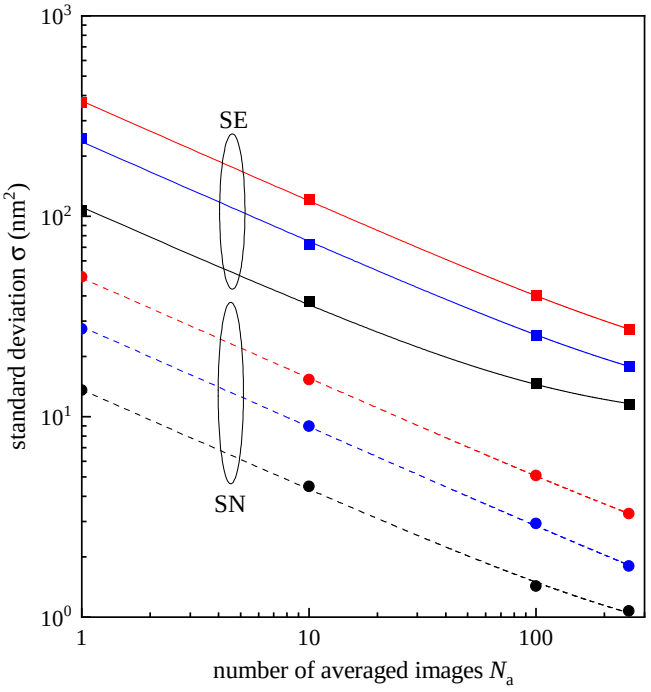

FIG. S22. As Fig. S20, but for the 1.27 NA objective.

dependence using the 1.45NA oil objective on a sample mounted in water oil.

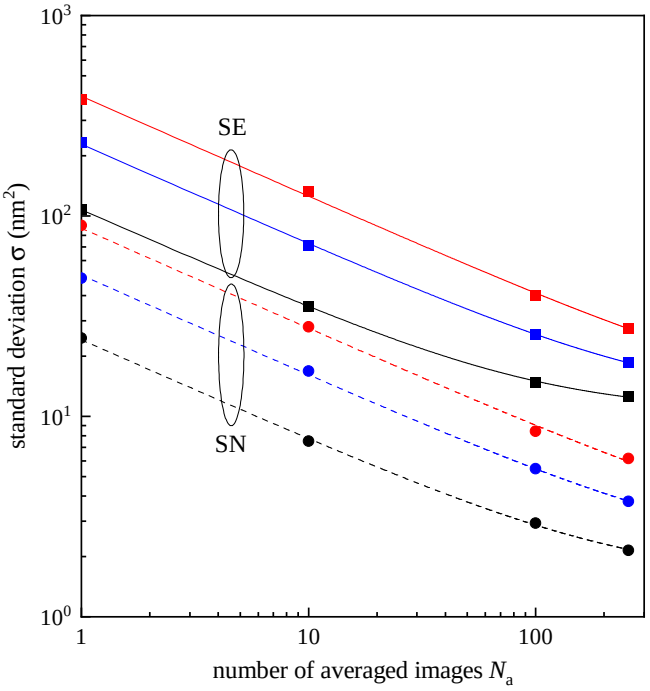

FIG. S23. As Fig. S20, but for the 1.27 NA objective with the water oil mounted sample.

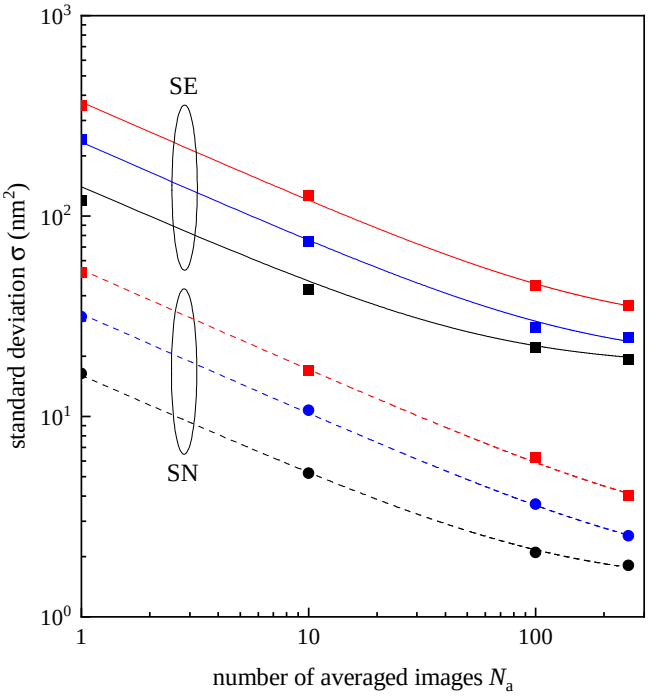

FIG. S24. As Fig. S20, but for the 1.45 NA objective with the water oil mounted sample.

TABLE S1. Table showing the median counts obtained for the different objectives and phase offsets ϕ, and the resulting background fraction f using Eq. S7 and background transmission factor η using Eq. S8, and the averege of η for each objective, $\bar{\eta}$.

ψ	$\langle I_0 \rangle$	$\langle I_{+\psi} \rangle$	$\langle I_{-\psi} \rangle$	$\langle I_{\psi} \rangle$	f	η (%)	$\bar{\eta}$ (%)
0.75 NA Objective							
30	48.82	467.54	401.70	434.62	0.13	0.89	0.86
60		1524.29	1306.77	1415.53	0.04		
90		2898.64	2449.13	2673.89	0.02		
20	95.83	501.61	429.02	465.32	0.26	0.86	
30		891.65	764.52	828.09	0.13		
60		2904.75	2461.42	2683.08	0.04		
10	307.74	655.61	517.93	586.77	1.10	0.85	
20		1597.09	1346.04	1471.56	0.26		
30		2808.64	2313.66	2561.15	0.14		
10	573.249	1220.24	953.61	1086.93	1.12	0.83	
20		2780.06	2648.03	2714.05	0.27		
1.27 NA Objective							
30	37.33	441.54	404.11	422.83	0.10	0.68	0.64
60		1475.73	1366.07	1420.90	0.03		
90		2865.59	2523.26	2694.43	0.01		
20	72.30	465.95	426.96	446.46	0.19	0.64	
30		836.83	787.66	812.24	0.10		
60		2795.25	2517.54	2656.40	0.03		
10	253.68	592.30	555.38	573.84	0.79	0.63	
20		1536.80	1493.51	1515.15	0.20		
30		2810.12	2635.14	2722.63	0.10		
10	495.112	1139.14	1106.46	1122.80	0.79	0.61	
20		2817.31	2937.73	2877.52	0.21		
1.45 NA Objective							
30	46.77	444.16	406.59	425.37	0.12	0.87	0.80
60		1454.97	1297.56	1376.26	0.04		
90		2823.39	2417.96	2620.68	0.02		
20	90.87	477.74	428.47	453.11	0.25	0.82	
30		882.57	778.77	830.67	0.12		
60		2766.27	2502.96	2634.62	0.04		
10	299.38	659.17	579.45	619.31	0.94	0.77	
20		1546.78	1461.34	1504.06	0.25		
30		2786.52	2579.88	2683.20	0.13		
10	568.738	1221.61	1097.11	1159.36	0.96	0.75	
20		2809.55	2738.49	2774.02	0.26		
1.49 NA Objective							
20	411	2801	1467	2134	0.24	0.72	0.96
30	337	2717	1619	2168	0.18	1.2	

S6. SMALL PS BEADS

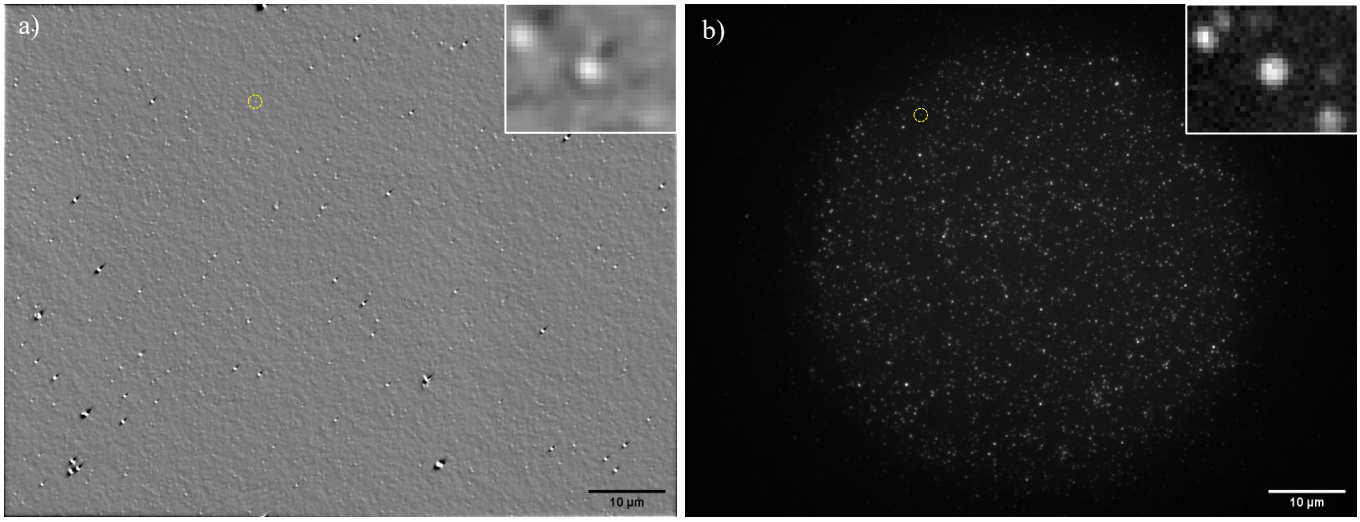

FIG. S25. (a) qDIC phase $\phi(\mathbf{r})$ on fluorescent PS beads of nominally 15 nm radius, drop cast onto glass and surrounded by water oil, imaged with a 1.49 NA objective at a phase offset of $\psi = 20°$ and analysed using $\kappa = 1$ and $N_a = 256$. Grey scale from $m = -1$ mrad to $M = 1$ mrad. The inset shows a region of $(2.07 \times 1.55)\,\mu m^2$ around a bead highlighted by the yellow dashed circle. This bead has an A_ϕ^m corresponding to a radius of 25 nm. (b) epi-fluorescence intensity I_{fl} (average of 5 frames with 3 s exposure time each) of the same sample region, on a greyscale from $m = 41$ to $M = 3717$ phe. The excitation area was limited to the discernible disk region by a field aperture. Inset as in (a), greyscale $m = 41$ to $M = 1417$ phe.

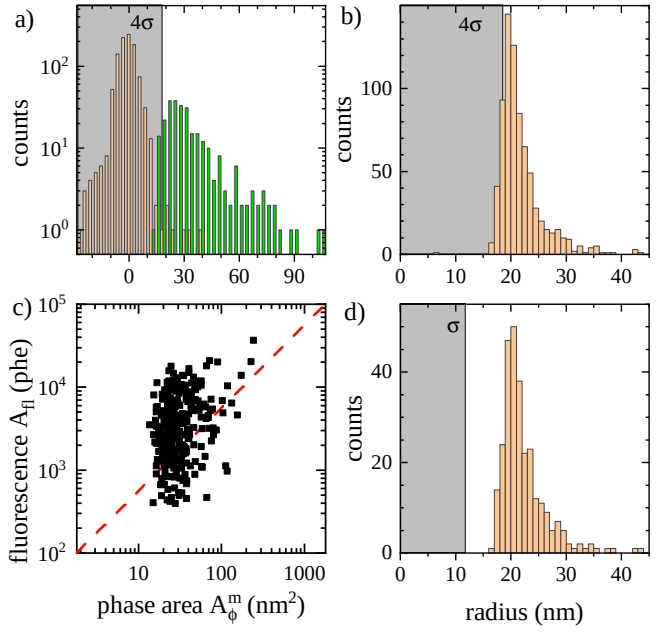

FIG. S26. Analysis of data shown in Fig. S25. (a) histogram of the phase area A_ϕ^m for background (orange, $\sigma = 4.6\,nm^2$), and particles (green) located as maxima in $\phi(\mathbf{r})$ above 0.33 mrad. The region below 4σ is indicated in gray. (b) resulting histogram of particle radius. (c) fluorescence photoelectrons A_{fl} versus A_ϕ^m, with a proportionality indicated as dashed line. (d) histogram of particle radius with corresponding A_{fl} above 455 phe.

S7. NANODIAMONDS

All nanodiamonds imaged were purified by immersing them in sulfuric acid for 2 hours, followed by air annealing at 600°C for 5 hours. Fig. S27 and Fig. S28 show the δ and ϕ images of the 0 - 250 nm NDs and 0 - 150 nm NDs, respectively, using the 0.75 NA objective at $\psi = 30°$. Fig. S29 shows the δ and ϕ images of the 0 - 50 nm NDs using the 1.27 NA objective at $\psi = 60°$.

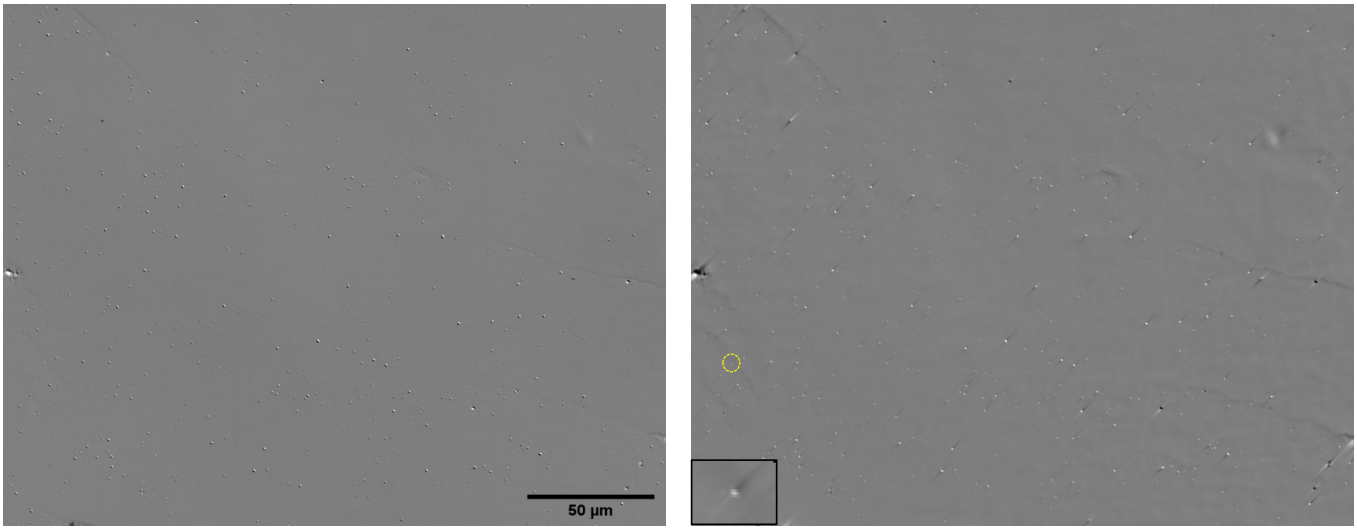

FIG. S27. qDIC on the 0 - 250 nm ND sample in silicon oil imaged with 0.75 NA and a phase offset of $\psi = 30°$. Left: $\delta(\mathbf{r})$ on a grey scale as shown in Fig. S5, from $m = -31.3$ mrad to $M = 31.7$ mrad. Right: corresponding $\phi(\mathbf{r})$ for $\kappa = 100$ ($m = -51.9$ mrad to $M = 53$ mrad). Note the presence of a few dark contrast spots, which are likely gas bubbles. The inset shows a region of $(6.92 \times 5.19)\,\mu\text{m}^2$, from $m = -30$ mrad to $M = 30$ mrad, around a particle highlighted by the circle, of approximately average size for the ND sample shown ($V = 4.18 \times 10^5\,\text{nm}^2$, $S = 74.7$ nm) .

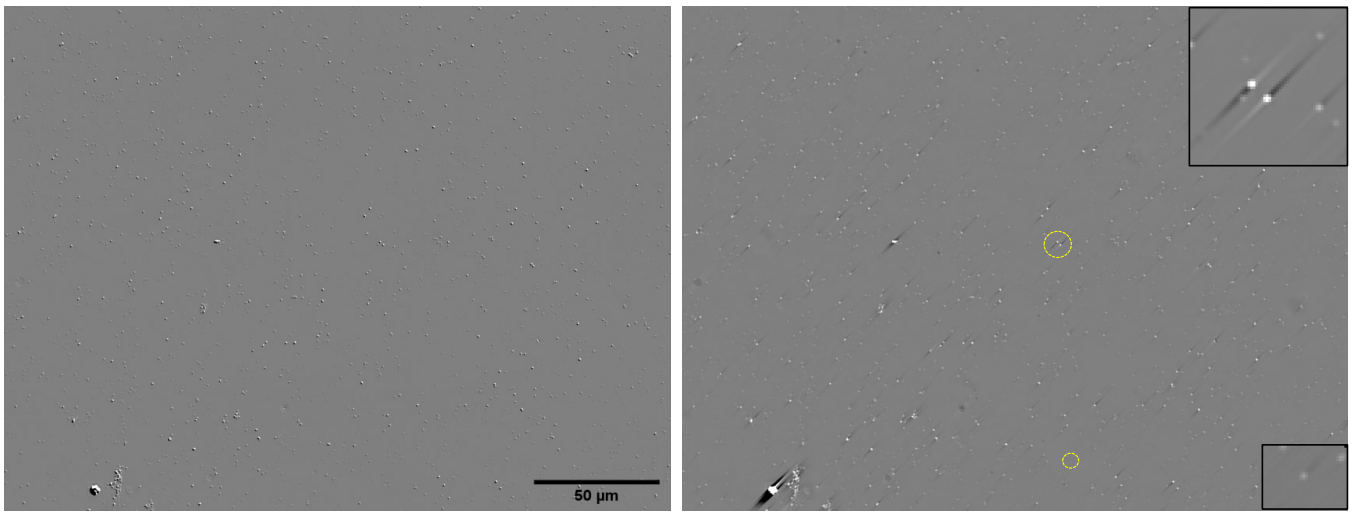

FIG. S28. As Fig. S27, but for the 0 - 150 nm ND sample, and scales left $m = -30$ mrad to $M = 30$ mrad, right $m = -50$ mrad to $M = 50$ mrad. The bottom inset shows a region of $(6.92 \times 5.19)\,\mu\text{m}^2$, highlighted by the lower circle, from $m = -30$ mrad to $M = 30$ mrad, around a particle of approximately average size for the ND sample shown ($V = 2.4 \times 10^5\,\text{nm}^2$, $S = 62.1$ nm). The top inset shows a region of $(13 \times 13)\,\mu\text{m}^2$ containing two particles, highlighted by the upper circle, of opposite asymmetry of the tails.

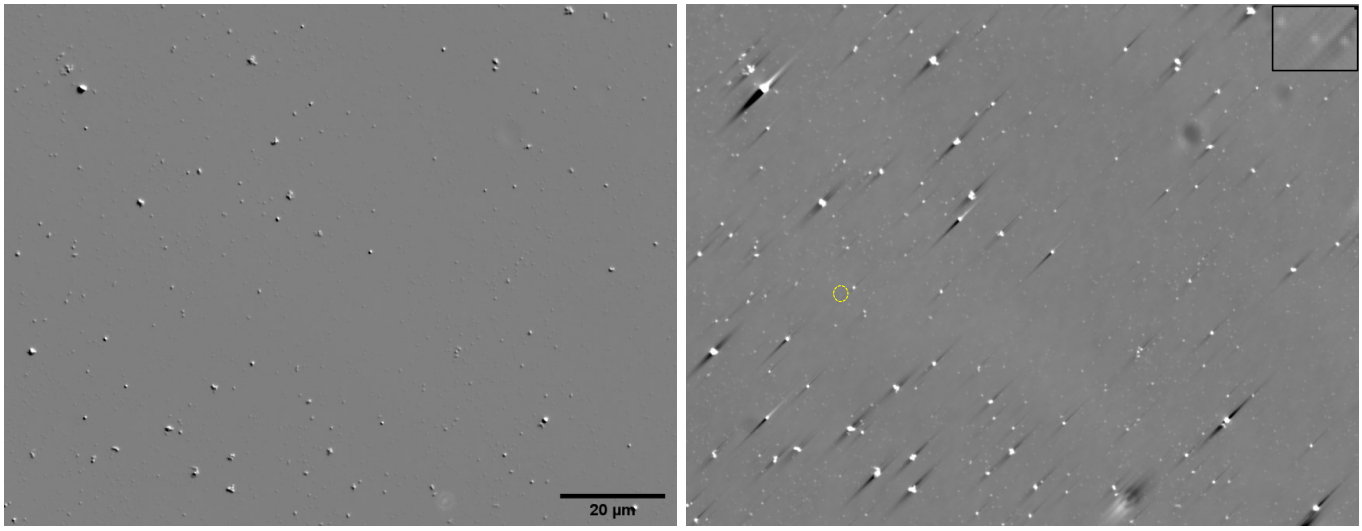

FIG. S29. As Fig. S27, but for the 0 - 50 nm ND sample , and scales left $m = -50$ mrad to $M = 50$ mrad, right $m = -30$ mrad to $M = 30$ mrad. The inset shows a region of $(3.65 \times 2.58)\,\mu\text{m}^2$, from $m = -10$ mrad to $M = 10$ mrad, around a particle highlighted by the circle, of approximately average size for the ND sample shown ($V = 2.1 \times 10^4\,\text{nm}^2$, $S = 27.6$ nm).

S8. SOFTWARE AND ANALYSIS PROCEDURE

This procedures describes how to analyse DIC images using both the qDIC v2.22 and Extinction Suite software.

i. qDIC V2.22

This software (http://langsrv.astro.cf.ac.uk/qDIC) is used to obtain ϕ and δ images from the initial positive and negative phase angle image stacks.

- Ensure image stacks have been averaged using the z project function in imagej.
- Save these images as img_000000000 in folders labelled as either 'p' or 'm'.
- The background for these stacks can be obtained in one of two ways:
  - A background stack of a clean region obtained at 0 degrees phase angle can also be included, labelled in the same way, in a folder labelled 'b'.
  - Alternatively the background can be calculated using the equation $\langle I_{\pm}^{\mathrm{m}} \rangle 2\eta/(1-\cos(\psi))$,
    - $\langle I_{\pm}^{\mathrm{m}} \rangle$ is the average intensity found from the positive and negative images.
    - η is dependant on the objective which is 0.86% for the 0.75 NA objective, 0.64% for the 1.27 NA objective, and 0.80% for the 1.45 NA objective.
    - ψ is the phase angle and is twice the polariser angle.
- The objective NA, and pixel size were also dependant on the objective and tube lens used.
  - 20× objective with 1.5× tube lens: NA = 0.75, Pixel size = 216.1 nm.
  - 60× objective with 1× tube lens: NA = 1.27, Pixel size = 107.4 nm.
  - 100× objective with 1× tube lens: NA = 1.45, Pixel size = 64.6 nm.
- For all measurements with this setup, the shear vector magnitude = 238 nm, and shear vector direction = -45 degrees.
- For this experiment a mean wavelength of 550 nm was used.
- k-filter factor was set to 0.2.
- The signal to noise ratio parameter (κ) was varied throughout the experiment to find the best values to use for each objective:
  - 0.75 NA objective
    - SN pair – 1
    - C pair – 10000
    - SE pair – 100
  - 1.27 NA objective
    - SN pair – 1
    - C pair – 1000
    - SE pair – 100
  - 1.45 NA objective
    - SN pair – 1
    - C pair – 1000
    - SE pair – 200
  - After running the software, a folder labelled 'out' is produced in which the resulting delta and phi images can be found.

ii. Extinction Suite V4.15

This software (http://langsrv.astro.cf.ac.uk/Crosssection) is used to obtain the integrated phase area, and hence volume and radius of the particles, from the ϕ image produced by the qDIC v2.22 software.

- Open the phi.dat file using imagej and save as a tif file called Extinction_550 in a folder labelled 'ProcessedImages'.
  - If a different wavelength is used, change the name of the file accordingly, e.g Extinction_500 for a mean wavelength of 500 nm.
- Run the Extinction Suite software as an imagej macro.
- Select the 'Unpolarized' analysis mode and the operation 'Run Extinction Suite'.
- Select the option 'Perform Particle Analysis'.
- Select the Base folder in which the ProcessedImages folder can be found.
- If a prior analysis has been made and a Processing file is in the Base folder, the option to use the same parameter will be available to use:
  - Selecting this option will automatically analyse the image using the same parameter as have been used before saved in the Prcocessing folder.
  - If no such analysis has been performed, or if different parameters are to be used, unselect this option to continue the analysis.
- The analysis options can now be selected, for this experiment the following parameters were used:
  - Colour channel – 550

  - Input ranks of channels – 1
  - Total number of brightfield images – 512 (256 positive and 256 negative)
  - Analysis route – Extinction
  - Background subtraction method – Defocus
  - Proximity restriction – 2
  - Number of BG datapoints – 1000
  - Numerical aperture and magnification depended on the objective
    * 0.75 NA - 30×
    * 1.27 NA - 60×
    * 1.45 NA - 100×
  - Pixel size of the camera – 6.45 µm.
  - Full well capacity - 18000
- For additional analysis options:
  - N – 1000
  - Radius of ROI (r_i) depends on the objective and κ value used.
    * 0.75 NA, SN pair – 1
    * 0.75 NA, C pair – 4
    * 0.75 NA, SE pair – 2
    * 1.27 NA, SN pair – 1.5
    * 1.27 NA, C pair – 8
    * 1.27 NA, SE pair – 2
    * 1.45 NA, SN pair – 2.5
    * 1.45 NA, C pair – 8
    * 1.45 NA, SE pair – 4
  - Outer radius is selected as $2r_\mathrm{i}$
- The ROI format selected was rectangle and determines the region in which particles will be analysed.
- To determine which prominence to use, use the find maxima funtion in imagej to find the value that selects all particles observable in the region selected. Make sure not to select the particles using the find maxima function, but enter the value found into the noise tolerance window.
- The software will then run and analyse the points selected, as well as the specified number of background points.
- A histogram showing the number of particles found at given values of integrated phase area (In this software given as Sigma).
  - The plot can be redisplayed with a given number of bins, which can be selected to give the best view of the data.
  - Once happy with the number of bins, change the redisplay histogram option to display 'No'.
- At this point the choice of which region of the histogram to save as filtered particles can be selected.
- Folders labelled at 'Processing', and 'Results'.
  - The 'Processing' folder contains files to be used if the same parameters are to be used again. The parameters can be changed in the parameters.txt file if anything needs to be changed for the data to be reanalysed.
  - The 'Results' folder contains the filtered and unfilterd particle results, as well as the filtered and unfiltered particle histograms, and the background results.
- In the filtered particles file, can be found the results from each particle with their x and y positions in the image, and the integrated phase (again given as Sigma).
  - To find the volume, calculate the difference in refractive index between the sample and medium, e.g. $n_\mathrm{p} - n_\mathrm{m} = 1.59 - 1.334 = 0.256$ between PS beads and water oil.
  - The volume can then be found using $V = \frac{A\lambda}{2\pi(n_\mathrm{p}-n_\mathrm{m})}$.
  - At this point the correction factor associated with the objective and which set of κ and r_i used can be applied to the volume.
  - The radius of the particles can then be found, $R = \sqrt[3]{\frac{3V}{4\pi}}$.

[1] N. Farkas and J. A. Kramar, Dynamic light scattering distributions by any means, J. Nanopart. Res. **23**, 120 (2021).